RSC Advances

Comparative study of dry-mixing and wet-mixing activated carbons prepared from waste printed circuit boards by NaOH activation

Yujiao Kan, Qinyan Yue*, Baoyu Gao, Qian Li

Shandong Provincial Key Laboratory of Water Pollution Control and Resource Reuse, School of Environmental Science and Engineering, Shandong University, Jinan 250100, China

* Corresponding author. Tel: +86 531 88365258; fax: +86 531 88364513

E-mail address: qyyue58@aliyun.com

Abstract: Two activated carbons have been produced from non-metallic fraction (NMF) of waste printed circuit boards (WPCB) by sodium hydroxide activation in two methods, dry-mixing and wet-mixing. Dry-mixing is the waterless way by direct powder maceration, activated carbon prepared through this way is called AC. Wet-mixing is by impregnation within an aqueous solution, activated carbon prepared through this way is called WAC. Activated carbons differed with the physical structure and chemical properties which were derived from N_2 adsorption/desorption isotherms and Fourier-transform infrared spectroscopy (FTIR). Batched sorption studies were performed to compare the ciprofloxacin (CIP) adsorption properties of the two carbons. Experiments proved that the method of mixing has great influence on the preparation of activated carbons, AC showed better characteristics and adsorption properties than WAC. AC had 2304 m^2/g of surface area, while WAC had 1141 m^2/g of surface area. Fourier transform infrared spectra indicated two activated carbons had similar functional groups. For both adsorbents, the adsorption kinetics followed the pseudo-second-order model. The adsorption equilibrium data were very well represented by Langmuir equations.

Keywords: waste printed circuit boards; activated carbons; dry-mixing; wet-mixing; carbonation; NaOH

1. Introduction

With the phenomenal advancement and growth in electronic industries, much demands for electric and electronic equipments (EEE) make the replacement of electronic equipments more frequent, resulting in large amounts of electronic waste (E-waste) to be disposed of [1]. Current estimate shows nearly 45 million tons of E-waste is generated globally per annum and the number is growing at an exponential rate [2].

Waste printed circuit boards (WPCB) are one of the most complicated constituents of WEEE. WPCB, which contains valuable resources together with some hazardous materials, are thus considered to be an attractive secondary resource and an environmental contaminant [3]. In order to recycle the valuable resources, hydrometallurgical process which includes various steps of leaching, separation and purification is the main route [4, 5]. Unfortunately, toxic water would be generated during these procedures. Novel approaches to reuse WPCB are urgently to be proposed. Because of the high content of organic compounds in non-metallic fraction (NMF) of WPCB [6], it can be used as a low-cost raw material for preparing activated carbons. Researches focused on the preparation of activated carbon from WPCB are few [7,8].

Activated carbon can be prepared by different activating agents. The use of alkali hydroxides(NaOH, KOH) for the production of microporous activated carbons has attracted great interest due to the valuable properties of the materials produced by this process. Compared with KOH activations, NaOH activation has advantages such as: (I) lower dosage; (II) cheaper; (III) more environmentally; (IV) less corrosive [9]. Another reason is that NaOH occurs carbonation in the presence of water. Different mixing ways

may display different reactions, which has great influence on the preparation of activated carbon. For the reason above, we choose NaOH as the activating agents.

Ciprofloxacin (CIP) is a synthetic antibiotic widely used for the treatment of several bacterial infections that can end up into water courses due to incomplete metabolism in humans or coming from effluents of drug manufacturers. The presence of CIP in water sources can lead to the development of antibiotic resistant bacteria, which is extremely harmful to the health of the human [10]. Thus, removing CIP from water has become an increasingly important subject. Various methods including adsorption [11], degradation [12] and oxidation [13] had been studied for removing CIP. Adsorption is considered the most suitable treament because it inhibits the toxic properties and restricts the transportation into water systems [14].

This study focused on comparison of dry-mixing and wet-mixing to prepare NMF-based activated carbons by NaOH activation. Dry-mixing is the waterless way by direct powder maceration, activated carbon prepared through this way is called AC. Wet-mixing is by impregnation within an aqueous solution, activated carbon prepared through this way is called WAC. The two activated carbons differed with the physical structure and chemical properties which were derived from N_2 adsorption/desorption isotherms and Fourier-transform infrared spectroscopy (FTIR). Batched sorption studies were performed to compare the CIP adsorption properties of AC and WAC. Experiments proved that the method of mixing had great influence on the preparation of activated carbons, and AC showed better characteristics and adsorption properties than WAC.

2. Materials and methods

2.1. Materials

The non-metallic powders were provided by Shandong Zhonglv Eco-recycle Co., Ltd. The properties of the raw materials were represented in Fig.1. All chemical reagents

used in this study were analytical grade. CIP ($C_{17}H_{18}FN_3O_3$) was purchased from Sangon

Biotech (Shanghai, China) Co., Ltd.

2.2. Preparation of AC and WAC

First, a carbon-rich carbonized sample was prepared from the pyrolysis of the raw

materials under N_2 atmosphere at 600 °C for 2 h. The carbonized sample was solid powder

with size lower than 0.25 mm (60 mesh) diameter. Next, the carbonized sample was

mixed with NaOH by two different processes: dry-mixing or wet-mixing. The progress

flow charts had been showed in Fig.2.

In the dry-mixing, sodium hydroxide powders are directly mixed with a given

amount of the carbonized sample. It should be emphasized that the process is done in

absence of water.

In the wet-mixing, the carbonized sample was mixed with sodium hydroxide adding

10mL distilled water. Then stirring often to make sure the sodium hydroxide dissolved

completely. After the impregnation process, the mixtures were dried at 110°C for 5 h.

For the two preparation methods, dry-mixing or wet-mixing, the NaOH/carbonized

sample weight ratio was kept equal to 3:1. The activation heat-treatments were conducted

under N_2 flow at 800 °C for 1 h in a cylindrical furnace. After the heat treatment, a

washing process was carried out by using a 2 M HCl solution firstly, and afterwards

washed with distilled water until the pH value reached to neutral. Then, carbons were

dried at 110 °C for 4 h, ground and sieved by sieves to 0.147 mm. The carbon prepared by

dry-mixing was named as AC. The carbon prepared by wet-mixing was named as WAC.

2.3. Characterization methods

SDT Q600 equipment was used to obtain thermo gravimetric analysis (TGA) and differential scanning calorimetry (DSC) diagram. Scanning electron microscope (SEM, Hitachi S-520) was used to study the changes in surface morphology. The BET surface area (S_{BET}) and porous properties of AC and WAC were determined by N_2 adsorption/desorption isotherms at 77 K using a surface area analyzer (Quantachrome Corporation, USA). The S_{BET} and the total pore volume (V_{tot}) were obtained by the manufacturer's software. The S_{BET} was derived from the Brunauer–Emmett–Teller (BET) theory. The micropore surface area (S_{mic}), external surface area (S_{ext}) and the micropore volume (V_{mic}) were evaluated by the t-plot method. The pore size distribution was obtained by the Density Functional Theory (DFT) method. The mean pore diameter (D_p) was obtained from $D_P = 4V_{tot}/S_{BET}$. The surface functional groups of AC and WAC were recorded by the KBr technique using a Fourier transform infrared (FTIR) spectrometer (Fourier-380FT-IR, USA), and the spectra were recorded in the spectral range 4000–400 cm^{-1}.

2.4. Adsorption procedure

Parallel series of batch adsorption tests were carried out in conical flask with cap containing AC or WAC. In both of them, 0.05 g of solid adsorbent was introduced to 50 mL solution containing a specific amount of CIP (200-800 mg/L). All pH measurements were carried out using a pH meter (Model pHS-3C, Shanghai, China). The initial pH levels of the experimental solutions were adjusted to constant values by adding various concentrated HCl or NaOH solutions. The flasks were then transferred to a water-bath thermostatic shaker (SHA-B, Shanghai, China) at determined temperature and shook at

170 rpm for 24 h to ensure that the adsorption process reached equilibrium. One conical

flask containg 50mL CIP solution sample was taken off at various time intervals to

determine adsorption kinetics. Samples were filtered using a 0.45μm membrane filter, and

the CIP concentration of the filtrate was analyzed using UV/Vis spectrophotometer

(UV-754, Shanghai) at the maximum wavelength of 275 nm.

2.5. Adsorption isotherm and kinetic models

In order to explain the adsorption mechanism, the kinetic data were analyzed with

pseudo-first-order [15], pseudo-second-order [16], Elovich [17] and intra-particle diffusion

models [18]. Similarly, the isothermal data were analyzed with Langmuir [17], Freundlich

[19] and Tempkin models [20]. The kinetic and isotherm models were listed in Table 1. The

determination coefficient (R^2) and normalized standard deviation (Δq_e) were evaluated to

define which models best describes the experimental data. Δq_e was calculated using the

following equation [20]:

$$\Delta q_e(\%) = 100 \times \sqrt{\frac{\Sigma[(q_{e,\exp} - q_{e,cal})/q_{e,\exp}]^2}{N-1}}$$

(1)

Where N is the number of experimental data points.

3. Results and discussion

3.1. Thermal analysis

The two samples were prepared by dry-mixing or wet-mixing, respectively. Both of

them were heated between 20 and 800 °C under N_2 atmosphere. The thermal analyses are

illustrated in Fig.3. The pyrolysis process can be divided into three steps: an initial weight

loss due to the evaporation of moisture (a: 5.19%; b: 12.58%), a significant mass loss in

200-500 °C, which was the main weightlessness area for the precursors (a: 27.86%; b:

22.31%), benzene reacted with NaOH to form new structures resulting in the loss of

organic compounds. A slow mass loss at the last stage between 500 and 800 $^{\circ}$C (a: 8.43%;

b: 6.49%), confirming the stable structure of the resultant char was formed in this

temperature range. Because of the different mixing method, the thermal analyses of two

samples in the three mass loss stages have significant differences, especially in the first

stage, since the precursor of WAC have higher moisture content that the precursor of AC.

The carbon-rich carbonized sample was prepared from the pyrolysis of the

non-metallic powders under N_2 atmosphere at 600 $^{\circ}$C for 2 h. The main reaction process

was showed in Fig.4. The first step of the decomposition process is the release of water

and the formation of unsaturated structure. For the structure I, when C-O and C-Br were

broken, bisphenol A (BPA) would be generated. For the structure II, the extraction of H

resulted in the formation of phenol. Structure II reacted with NaOH under different

conditions. The main reactions were showed as follows [21]:

$$2 \quad \underset{H_2}{C} \quad + \quad 6NaOH \quad \longrightarrow \quad 2Na \quad + \quad 5H_2 \quad + \quad 2Na_2CO_3$$

$$\underset{H}{C} \quad + \quad 3NaOH \quad \longrightarrow \quad Na \quad + \quad 2H_2 \quad + \quad Na_2CO_3$$
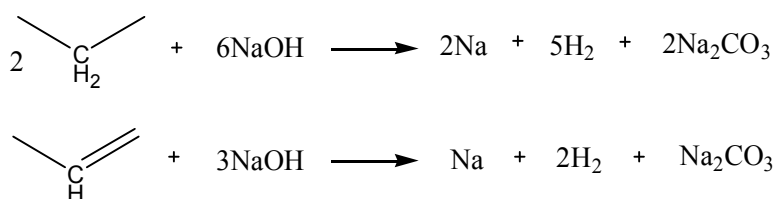
3.2 SEM analysis

The SEM profiles of AC and WAC were presented in Fig. 5. Both the samples had a

significant difference in appearance. The fragmentation degree of AC was higher than that

of WAC. The activating agents-NaOH played a bigger role in the dry-mixing than in the

wet-mixing. During the wet-mixing, part of NaOH occured carbonation, which prevent

the development of porosity. The porosity of two samples was related to the volatile

matter and gas generated in the activation progress.

3.3 Textural structure

The N_2 adsorption/desorption isotherms at 77 K has been determined in AC and WAC to assess their porous texture, which conclude pore volume, pore area and average pore diameter. Fig. 6 and Fig. 7 show the N_2 adsorption/desorption isotherms and pore size distributions, respectively. The structural parameters of AC and WAC were summarized in Table 2.

According to the classification of International Union of Pure and Applied Chemistry [22], the majority of physisorption isotherms can be grouped into the six types corresponding to six different types of pore structure. From Fig. 6, it can be seen that the N_2 adsorption/desorption isotherms for both adsorbents belongs to types I, corroborating that AC and WAC are microporous carbons. Additionally, the plateau showed nearly parallel to the axis of P/P_o, confirming the presence of micropores with no or few mesopores [23]. Compared with WAC, the pronounced increase in the volume of N_2 adsorbed and desorbed amount at the low pressure region of AC demonstrates the development of microporosity. In addition, the pore size distribution (Fig.7) of AC and WAC showed that a vast majority of the pores fall into the range of microspore.

As shown in Table 2, WAC showed a low S_{BET} in comparison to AC, probably because the amount of NaOH was not sufficient react with chars. When the materials containing NaOH and water are in air, thus, in a CO_2 atmosphere, the carbonation of the NaOH occurs (R.1), resulting in the reduction of NaOH. In the conditions of activation experiments (activation temperature of 800 $^{\circ}$C), the Na_2CO_3 is stable, is does not turn to any other sodium compound active for the activation, and therefore the carbonation of the

NaOH prevent the development of porosity. In another indication that the yield of WAC is

higher than that of AC [24].

The results above showed that AC has better porous characteristic than WAC. The

drying stage during the preparation of WAC is negative, lowering the development of

porosity [25].

$$2NaOH + CO_2 \leftrightarrow Na_2CO_3 + H_2O \hspace{3cm} (R.1)$$

3.3 Surface chemistry analysis

The adsorption abilities had much to do with the surface chemistry characteristic. In

order to understand the surface chemistry differences of AC and WAC, Table 3

summarizes the pH_{pzc} and number of surface functional group. The two adsorbents have

different values of surface acidity and basicity, which is represented as the amount of

acidic groups and basic groups, respectively. AC has higher pH_{pzc} value, smaller amount

of acidic functional group and larger amount of acidic functional group than WAC.

The FTIR spectrums of AC and WAC revealed different functional groups (Fig. 8).

The broad band at 3402 cm^{-1}, which could be attributed to the O–H stretching vibration

from OH^- groups (characteristic of NaOH) [23]. The peak at 1565 cm^{-1} is attributed to the

formation of oxygen functional groups such as C=O stretching in quinine structure [26]. The

bands at 1402 cm^{-1} are assigned to C–H bending in alkyl groups. The broad band between

1200 and 1000 cm^{-1} has been assigned to C–O stretching in alcohols and phenols [26]. This

part represented various configurations of C, O, H and N bonds in the carbon structures [27].

Seen from Fig.8, AC and WAC had very similar spectra, which confirmed that the

two samples had the similar functional groups on the surface. It indicated that the

activation mechanism of the two preparation methods were the same. Compared with AC, the intensity of the peaks at 3402 cm^{-1} in WAC reduced. In the initial reaction period for preparing WAC, the carbonation of the NaOH occurs, NaOH reacted with CO_2 to form Na_2CO_3, which weakened the intensity of the characteristic band of NaOH at 3402 cm^{-1} [25, 28].

3.4 Adsorption experiments

3.4.1 The effect of contact time and adsorption kinetics of CIP onto AC and WAC

The time required to reach the equilibrium in the adsorption study has been considered as a significant parameter. Fig. 9 illustrated the effects of contact time on the adsorption of CIP onto AC and WAC at 25 °C. The CIP concentration decreased rapidly in the first 4 h, and then the equilibrium was gradually obtained within 13 h. AC exhibit much better sorption and stronger adsorption affinity to CIP due to the larger surface area and total volume compared to WAC. This phenomenon implied that although adsorbent surface area and porous properties were the main affecting factors that affect the adsorption of CIP, other factor like the surface chemistry of adsorbents also may affect the adsorption.

The kinetic parameters were listed in Table 4. It can be seen the models of pseudo-first-order and Elovich were not suitable to describe the experimental data, presenting the lower R^2 (0.92-0.98) and the higher Δq_e values (3.05-10.29%). Instead, the pseudo-second-order model was well fitted to the experimental data with a higher R^2 (>0.99) and lower Δq_e value (<1.5%). The pseudo-second-order model assumed that the adsorption progress was affected by chemical interactions which lead to binding of the

adsorbate to the adsorbent surface as strong as covalent bonding, which was consistent

with the cation exchange and electrostatic attraction mechanism [18].

The intra-particle diffusion model assumed the adsoprtion mechanism occured

through the diffusion of the adsorbate molecules into the pores of adsorbent material [16].

The plots obtained for q_t versus $t^{1/2}$ were shown in Fig. 10. The parameters (k_{pi}, C_i and R^2)

were listed in Table 4. As can be seen in Fig. 10, all the adsorption data exhibit

multi-linear plots, illustrating that two or more steps influenced the adsorption process.

The first linear sections did not pass through the origin, which meant the intra-particle

diffusion was not the only rate-controlling step [29]. The first stage indicated external mass

transfer or external film resistance controlled the CIP adsorption. The second stage

described the gradual adsorption, where the intra-particle diffusion was the rate-limiting

step. The third stage was assigned to the equilibrium, where the intra-particle diffusion

started to slow down due to the extremely low concentration of CIP remaining in solution,

resulting in lower k_{pi} values for both stages [30].

3.4.2 Effect of pH

The adsorption of CIP onto AC and WAC as a function of pH had been shown in

Fig.11. The adsorption of CIP onto AC and WAC was pH-dependent. The main reason for

the change of adsorption capacity is the electrostatic interactions between adsorbent and

adsorbate [31]. The molecular structure of CIP is also an important factor to affect the

adsorption. CIP has three species (CIP^-, CIP^0, CIP^+) under different pH condition. CIP^+ is

the cationic form existing in the solution pH < 6.1, which is due to the protonation of the

amine group. CIP^0 is the zwitterionic form existing in the solution pH between 6.1 (pk_{a1})

and 8.7 (pk_{a2}), which contributes to balance the charge in the solution. CIP⁻ is the anionic

form existing in the solution pH > 8.7, which is due to a proton loss from the carboxylic

group [32]. The adsorption behavior should also be combined with the surface charge

characteristics of AC and WAC. The pH_{pzc} value of the two adsorbents were shown in

Table 3. The positively charged adsorbents gradually become negatively charged as the

pH value increases [33]. At solution pH < pk_{a1} (pk_{a1}=6.1), the CIP molecules and adsorbents

surface have opposite charges, thus adsorption is expected to be enhanced. When pH >

pk_{a2} (pk_{a2}=8.7), the amounts of CIP adsorbed onto adsorbents are expected to be

depressed, which was because CIP and adsorbents surfaces were negatively charged and

repelled each other [34]. The electrostatic effect for the sorption of CIP was shown in Fig.12.

3.4.3 Adsorption isotherm

Adsorption isotherms reflect the capacity of the adsorbents and the interaction

between adsorbents and adsorbates. The parameters of isotherm models for Langmuir,

Freundlich and Temkin were shown in Table 5. The Langmuir model described an

adsorption process that occurred upon a homogeneous surface where the adsorbate is

distributed in monolayers. According to the Table 5, Langmuir model showed higher

determination coefficient and lower normalized standard deviation than Freundlich and

Tempkin models, which indicating this adsorption process was monolayer coverage.

3.4.4 Adsorption thermodynamics

Thermodynamic parameters including changes in the standard Gibbs free energy

(ΔG), enthalpy (ΔH), entropy (ΔS), were determined by the following equations [35]:

$$\Delta G = - RT \ \ln \ K \tag{2}$$

$$\Delta G = \Delta H - T \Delta S \tag{3}$$

where R (8.314 J mol^{-1} K^{-1}) is the gas constant; T (K) is the absolute temperature; K (L mg^{-1}) is the Langmuir constant obtained from the plot of c_e/q_e vs. c_e .The values of ΔH and ΔS can be calculated from the slope and intercept of the plot of ΔG vs. T. From Table 6, the ΔG values for AC and WAC changed from -23.97 to -26.12 kJ/mol, -16.65 to -18.65 kJ/mol with the increasing temperature, respectively, indicating the adsorption of CIP onto AC and WAC were spontaneous and favorable process and they were more spontaneous at higher temperature. The positive value of ΔH confirms an endothermic nature of the adsorption process. The positive value of ΔS suggests the increased randomness at the solid/solution interface.
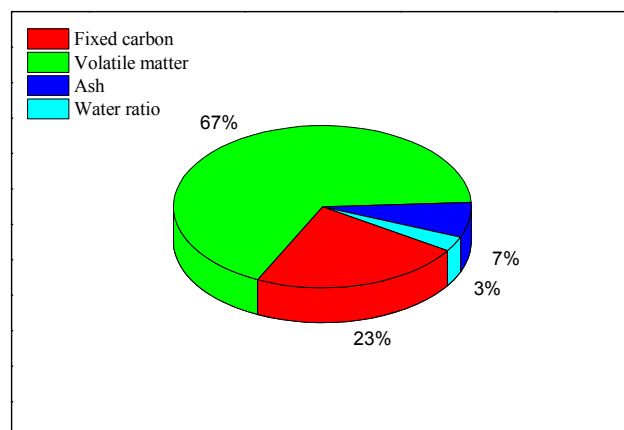
4. Conclusion

Two activated carbons have been produced from NMF of WPCB by sodium hydroxide activation in two methods, dry-mixing and wet-mixing. Dry-mixing is the waterless way by direct powder maceration, activated carbon prepared through way is called AC. Wet-mixing is by impregnation within an aqueous solution, activated carbon prepared through way is called WAC. AC had 2304 m^2/g of surface area and 1.171 cm^3/g of total pore volume, while WAC had 1141 m^2/g of surface area and 0.576 cm^3/g of total pore volume. Fourier transform infrared spectra indicated two activated carbons had similar functional groups. For both adsorbents, the adsorption kinetics followed the pseudo-second-order model. The adsorption equilibrium data were very well represented by Langmuir equations. Experiments proved that the method of mixing has great influence on the preparation of activated carbons, and AC showed better characteristics and adsorption properties than WAC.
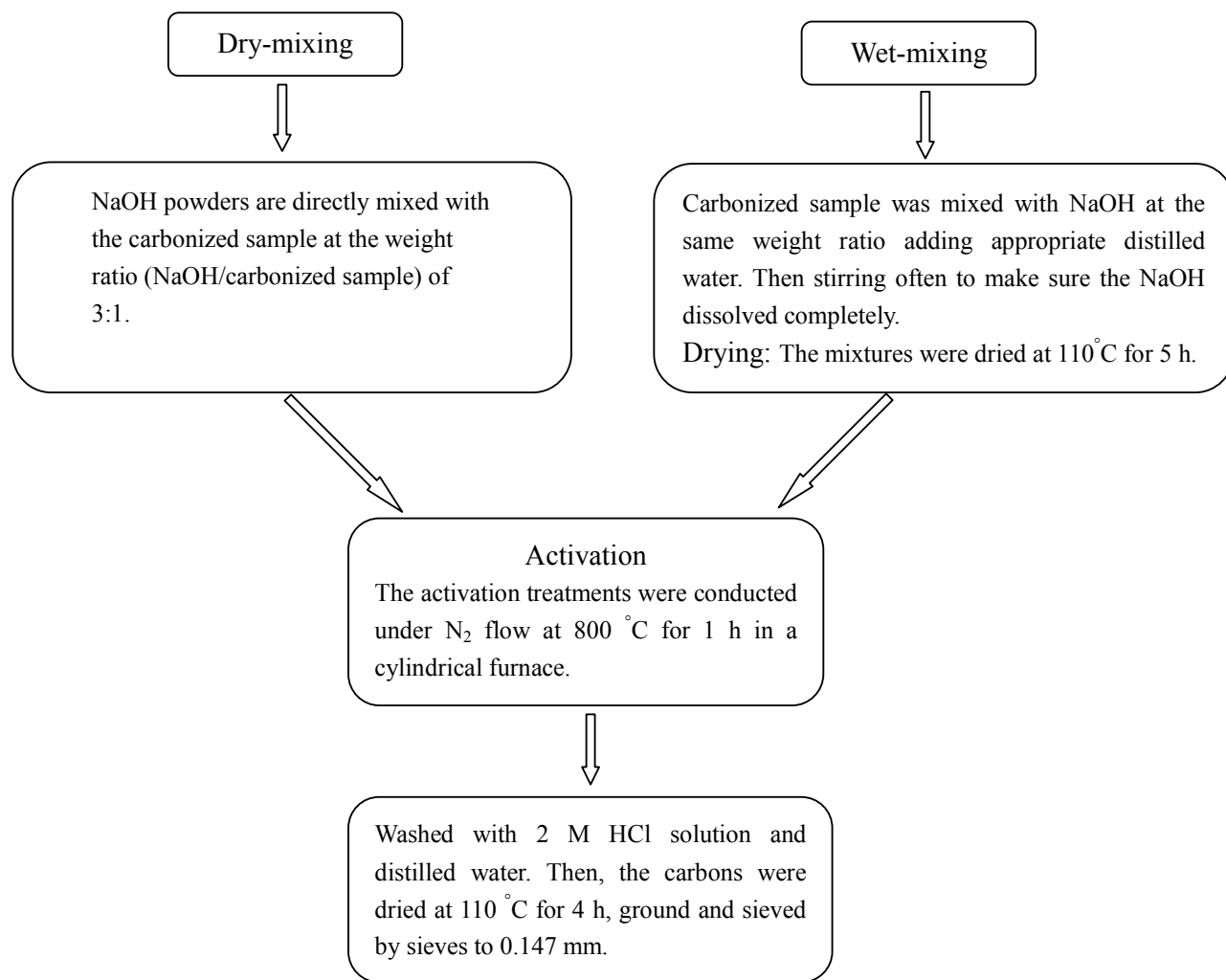
References:

1.   P. Hadi, C. Ning, W. Ouyang, M. Xu, C. S. K. Lin and G. McKay, *Waste Management*, 2015, **35**, 236-246.

2.   B. Ghosh, M. K. Ghosh, P. Parhi, P. S. Mukherjee and B. K. Mishra, *Journal of Cleaner Production*, 2015, **94**, 5-19.

3.   T. Hino, R. Agawa, Y. Moriya, M. Nishida, Y. Tsugita and T. Araki, *Journal of Material Cycles and Waste Management*, 2009, **11**, 42-54.

4.   Y. Zhang, S. Liu, H. Xie, X. Zeng and J. Li, *Procedia Environmental Sciences*, 2012, **16**, 560-568.

5.   I. Birloaga, I. De Michelis, F. Ferella, M. Buzatu and F. Vegliò, *Waste Management*, 2013, **33**, 935-941.

6.   Y. Kan, Q. Yue, J. Kong, B. Gao and Q. Li, *Chemical Engineering Journal*, 2015, **260**, 541-549.

7.   Y.-H. Ke, E.-T. Yang, X. Liu, C.-L. Liu and W.-S. Dong, *Carbon*, 2013, **60**, 563.

8.   J. Q. Zhang, S. H. Liu, J. H. Zu, C. Song and C. B. Yu, *Applied Mechanics and Materials*, 2014, **692**, 396-400.

9.   R.-L. Tseng, *Journal of colloid and interface science*, 2006, **303**, 494-502.

10.   A. C. Johnson, V. Keller, E. Dumont and J. P. Sumpter, *Science of The Total Environment*, 2015, **511**, 747-755.

11.   Y. X. Wang, H. H. Ngo and W. S. Guo, *Science of The Total Environment*, 2015, **533**, 32-39.

12.   H. Wang, J. Li, C. Ma, Q. Guan, Z. Lu, P. Huo and Y. Yan, *Applied Surface Science*, 2015, **329**, 17-22.

13.   P. Wang, Y.-L. He and C.-H. Huang, *Water Research*, 2010, **44**, 5989-5998.

14.   M. Brigante and P. C. Schulz, *Journal of hazardous materials*, 2011, **192**, 1597-1608.

15.   Y. X. Wang, H. H. Ngo and W. S. Guo, *The Science of the total environment*, 2015, **533**, 32-39.

16.   H. Liu, W. Liu, J. Zhang, C. Zhang, L. Ren and Y. Li, *Journal of hazardous materials*, 2011, **185**, 1528-1535.

17.   T. Aysu and M. M. Küçük, *International Journal of Environmental Science and Technology*, 2014, **12**, 2273-2284.

18.   B. H. Hameed, *Journal of hazardous materials*, 2009, **161**, 753-759.

19.   Y. Sun, Q. Yue, B. Gao, Q. Li, L. Huang, F. Yao and X. Xu, *Journal of colloid and interface science*, 2012, **368**, 521-527.

20.   A. C. Martins, O. Pezoti, A. L. Cazetta, K. C. Bedin, D. A. S. Yamazaki, G. F. G. Bandoch, T. Asefa, J. V. Visentainer and V. C. Almeida, *Chemical Engineering Journal*, 2015, **260**, 291-299.

21.   M. A. Lillo-Ródenas, J. Juan-Juan, D. Cazorla-Amorós and A. Linares-Solano, *Carbon*, 2004, **42**, 1371-1375.

22.   X. Wang, X. Liang, Y. Wang, X. Wang, M. Liu, D. Yin, S. Xia, J. Zhao and Y. Zhang, *Desalination*, 2011, **278**, 231-237.

23.   F. Rodriguez-Reinoso, *Pure and Applied Chemistry*, 1989, **61**, 1859-1866.

24.   E. Raymundo-Piñero, P. Azaïs, T. Cacciaguerra, D. Cazorla-Amorós, A. Linares-Solano and F. Béguin, *Carbon*, 2005, **43**, 786-795.

25.   M. A. Lillo-Ródenas, D. Cazorla-Amorós and A. Linares-Solano, *Carbon*, 2003, **41**, 267-275.

26.   P. Vinke, M. van der Eijk, M. Verbree, A. F. Voskamp and H. van Bekkum, *Carbon*, 1994, **32**, 675-686.

27.   M. M. Rao, D. H. Reddy, P. Venkateswarlu and K. Seshaiah, *Journal of environmental*
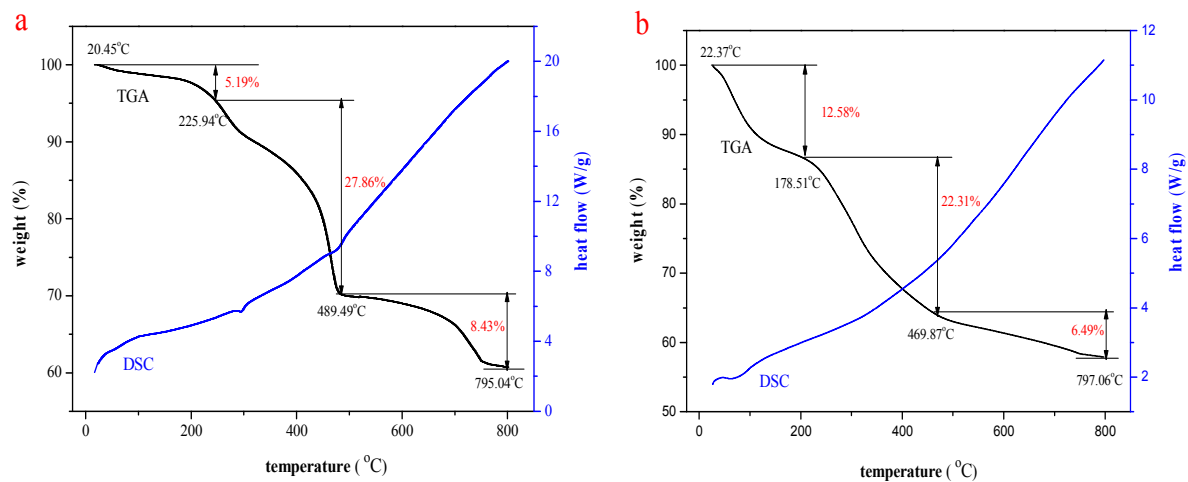
management, 2009, **90**, 634-643.

28. P. Zhu, Y. Chen, L. Y. Wang and M. Zhou, *Waste Management*, 2012, **32**, 1914-1918.

29. S. J. Allen, G. McKay and K. Y. H. Khader, *Environmental Pollution*, 1989, **56**, 39-50.

30. B. H. Hameed, I. A. W. Tan and A. L. Ahmad, *Chemical Engineering Journal*, 2008, **144**, 235-244.

31. S. A. C. Carabineiro, T. Thavorn-Amornsri, M. F. R. Pereira and J. L. Figueiredo, *Water Research*, 2011, **45**, 4583-4591.

32. Q. Wu, Z. Li, H. Hong, K. Yin and L. Tie, *Applied Clay Science*, 2010, **50**, 204-211.

33. S. A. C. Carabineiro, T. Thavorn-amornsri, M. F. R. Pereira, P. Serp and J. L. Figueiredo, *Catalysis Today*, 2012, **186**, 29-34.

34. Q. Wu, Z. Li, H. Hong, R. Li and W.-T. Jiang, *Water Research*, 2013, **47**, 259-268.

35. W. Liu, J. Zhang, C. Zhang, Y. Wang and Y. Li, *Chemical Engineering Journal*, 2010, **162**, 677-684.

Fig. 1. The properties of non-metallic powders.

Dry-mixing

Wet-mixing

NaOH powders are directly mixed with the carbonized sample at the weight ratio (NaOH/carbonized sample) of 3:1.

Carbonized sample was mixed with NaOH at the same weight ratio adding appropriate distilled water. Then stirring often to make sure the NaOH dissolved completely.

Drying: The mixtures were dried at $110\ ^{\circ}$C for 5 h.

Activation
The activation treatments were conducted under N_2 flow at 800 $^{\circ}$C for 1 h in a cylindrical furnace.

Washed with 2 M HCl solution and distilled water. Then, the carbons were dried at 110 $^{\circ}$C for 4 h, ground and sieved by sieves to 0.147 mm.

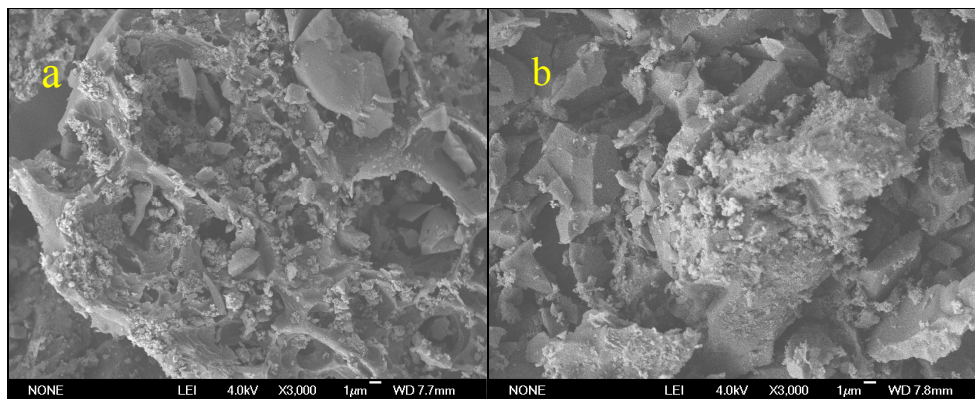**Fig. 2.** The progress flow charts of AC and WAC.

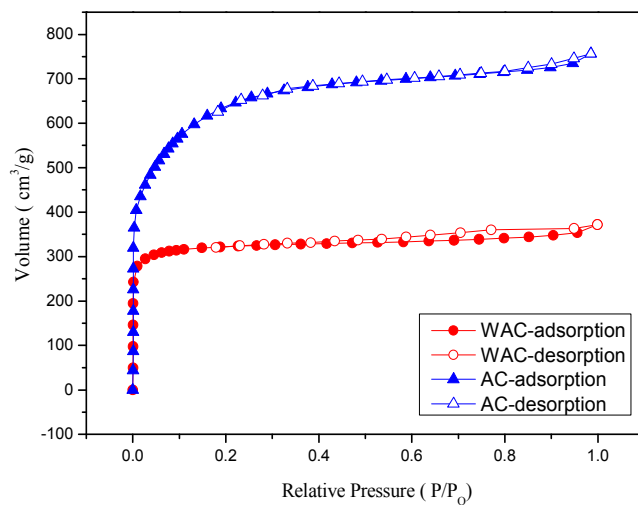**Fig. 3.** Thermal analysis (DSC/TGA) of dry-mixing (a) and wet-mixing (b)
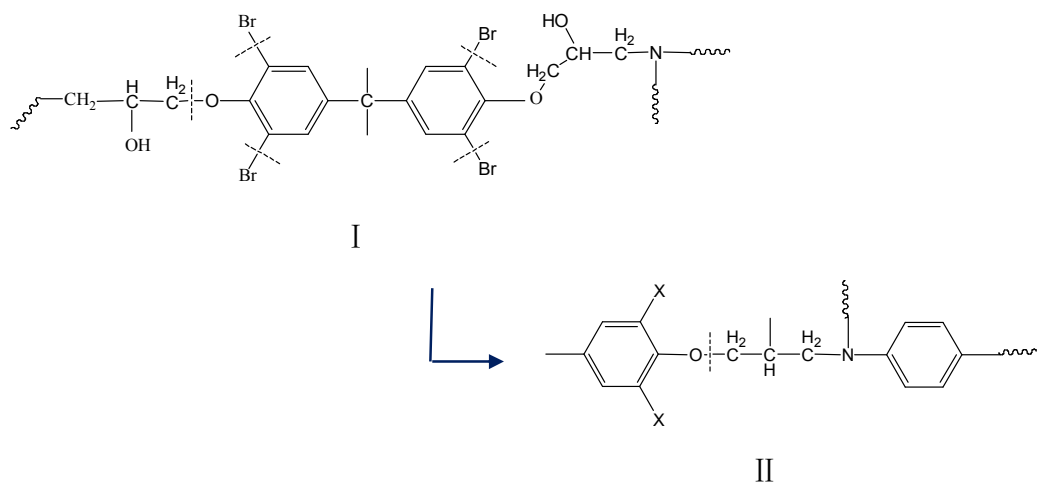
Fig. 4. The pyrolysis of epoxy resin monomer (I :the brominated epoxy resin monomer;

II :X is H or Br)

Fig. 5. SEM micrographs of (a) AC and (b) WAC.

Fig. 6. The adsorption-desorption isotherms of N_2 at 77 K for AC and WAC.
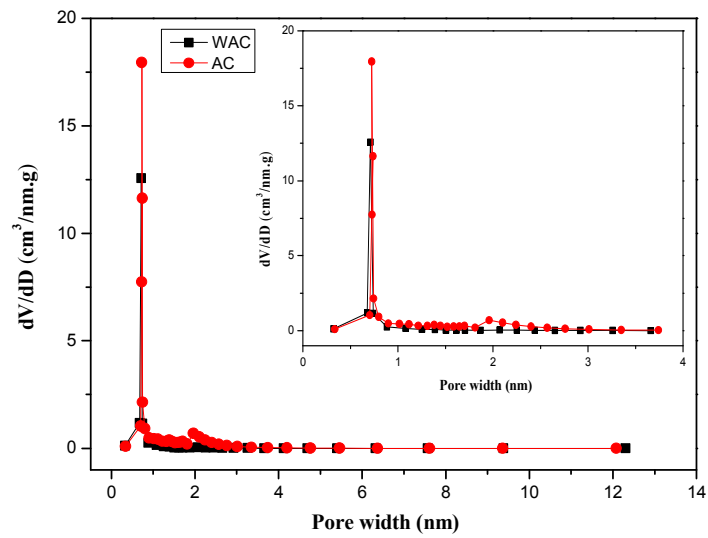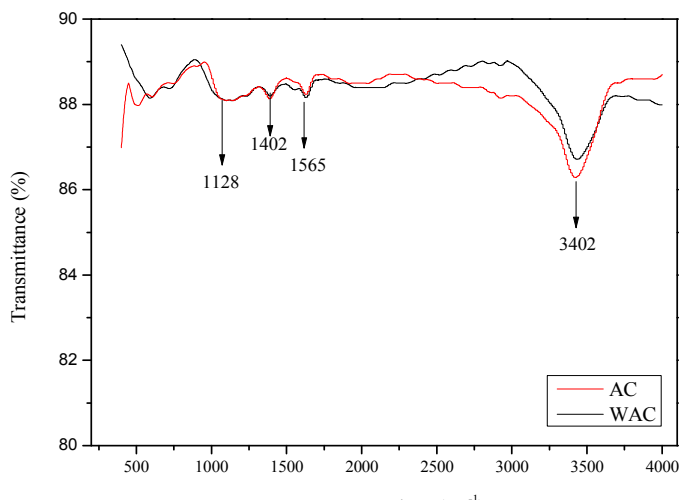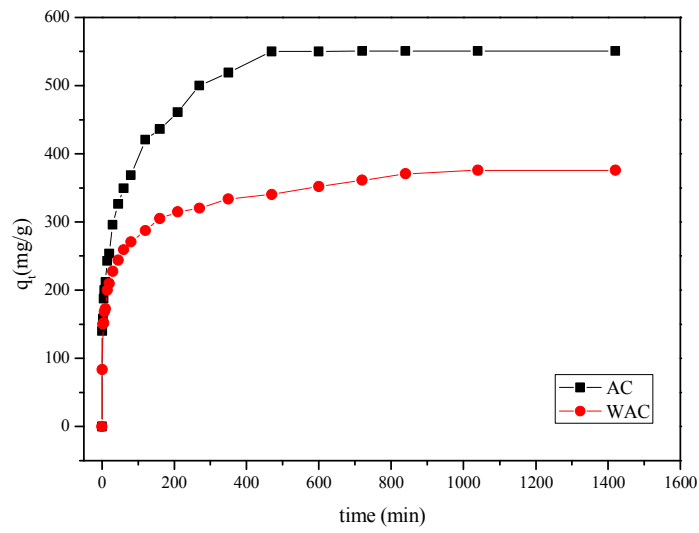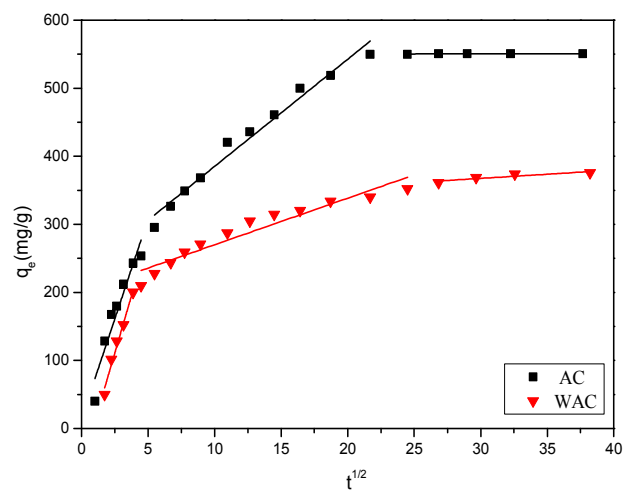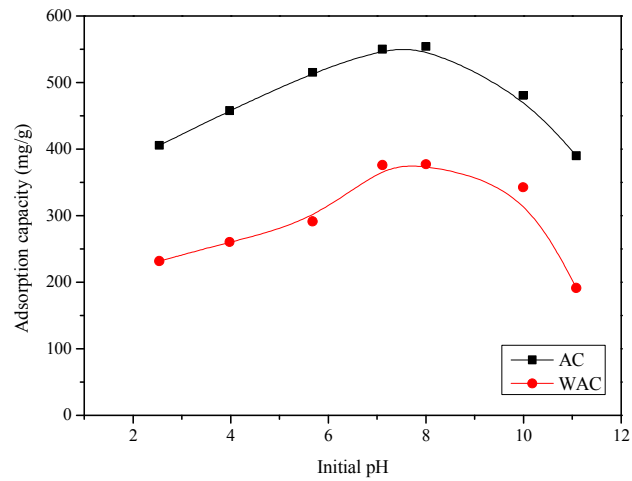
Fig. 7. Pore size distributions for AC and WAC.

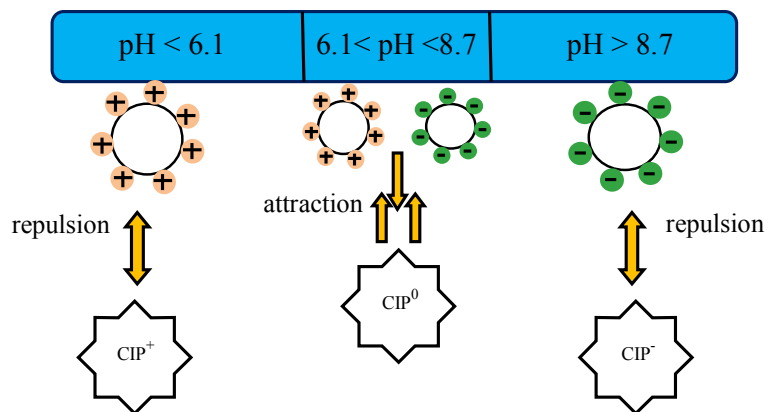**Fig. 8.** FTIR spectra of AC and WAC.

Fig. 9. Effect of contact time on CIP adsorption by AC and WAC.

Fig. 10. Intra-particle diffusion model for adsorption of CIP onto AC and WAC.

Fig. 11. The influence of solution pH on the adsorption of CIP onto AC and WAC.

Fig. 12. The electrostatic effect for the sorption of CIP.

Table 1

The kinetic models and isothermal models

Kinetic models	Names
$q_t = q_e(1 - e^{-k_1 t})$	Pseudo-first-order
$q_t = \dfrac{t k_2 q_e^2}{1 + t k_2 q_e}$	Pseudo-second-order
$q_t = \dfrac{1}{\beta} \ln(1 + \alpha \beta t)$	Elovich
$q_t = k_{pi} t^{1/2} + C_i$	Intra-particle diffusion
Isothermal models	**Names**
$q_e = \dfrac{q_m K_L c_e}{1 + c_e K_L}$	Langmuir
$q_e = K_F c_e^{\frac{1}{n}}$	Freundlich
$q_e = B_T \ln(K_T c_e)$	Temkin

q_t–adsorbed amount at any time; q_e–adsorbed amount at equilibrium; k_1–

rate constant of pseudo-first order model; k_2–rate constant of pseudo-second

order model; α and β –Elovich constants; k_{pi} and C_i–Intra-particle diffusion

constant; q_m–maximum adsorption capacity; K_L–Langmuir constant; K_F and

n –Freundlich constants; B_T and K_T–Temkin constants.

Table 2

Porous structure parameters of AC and WAC

Type	S_{BET}	S_{mic}	S_{mic}/S_{BET}	S_{ext}	S_{ext}/S_{BET}	V_{tot}	V_{mic}	V_{mic}/V_{tot}	V_{ext}	V_{ext}/V_{tot}	D_p	Yield
	(m^2/g)	(m^2/g)	(%)	(m^2/g)	(%)	(cm^3/g)	(cm^3/g)	(%)	(cm^3/g)	(%)	(nm)	(%)
AC	2304	1938	84.11	366	15.89	1.171	0.847	72.33	0.324	27.67	2.032	34.28
WAC	1141	1073	94.04	68	5.96	0.576	0.474	82.29	0.102	17.71	2.031	38.40

Table 3

The surface chemistry of AC and WAC

Acidic and basic funciton group concentration (mmol/g)

Samples	pH_{pzc}	Basic	Lactone	Carboxyl	Phenolic	Total acidic
AC	6.98	0.971	0.580	0.423	0.969	1.972
WAC	6.25	0.722	0.745	0.311	1.053	2.109

Table 4

Kinetic parameters for the adsorption of CIP onto AC and WAC

Kinetic models	Parameters	Adsorbent	
		AC	WAC
Pseudo-first-order	$q_{e,exp}$	550.72	375.74
	$q_{e,cal}$	394.26	195.02
	k_1	0.0043	0.0031
	R^2	0.9612	0.9267
	Δq_e	6.08	10.29
Pseudo-second-order	$q_{e,exp}$	559.91	380.22
	k_2	0.0024	0.0003
	R^2	0.9948	0.9986
	Δq_e	1.35	1.08
Elovich	α	437.55	286.78
	β	0.0234	0.0137
	R^2	0.9852	0.9790
	Δq_e	3.05	4.14
Intra-particle diffusion	k_{p1}	31.83	19.15
	C_1	112.3	117.2
	R^2	0.9921	0.9770
	k_{p2}	11.79	4.957
	C_2	286.3	236
	R^2	0.9381	0.9515
	k_{p3}	0.002	1.214
	C_3	550.6	331.2
	R^2	0.9592	0.8296

Table 5

Isotherm parameters for CIP adsorption onto AC and WAC

Isotherm models	Parameters	AC			WAC		
		298K	308K	318K	298K	308K	318K
Langmuir	q_m	572.11	586.29	603.84	381.29	406.72	429.65
	K_L	0.048	0.051	0.059	0.0025	0.0029	0.0035
	R^2	0.9963	0.9903	0.9969	0.9924	0.9942	0.9987
	Δq_e	0.89	1.17	0.87	1.09	0.93	0.75
Freundlich	K_L	297.10	301.72	315.94	176.67	184.99	195.26
	n	8.63	7.33	9.04	10.77	11.35	12.07
	R^2	0.9814	0.9774	0.9806	0.9733	0.9759	0.9853
	Δq_e	1.85	2.26	1.90	2.36	2.30	1.54
Temkin	K_T	9.874	14.098	21.767	7.176	8.7683	10.0481
	B_T	48.21	44.92	41.81	31.64	29.47	25.53
	R^2	0.9552	0.9822	0.9370	0.9339	0.9134	0.9005
	Δq_e	3.92	1.66	5.28	5.45	6.97	8.26

Table 6

Thermodynamic parameters for the adsorption of CIP on AC and WAC

Sample	T (K)	ΔG (kJ/mol)	ΔH (kJ/mol)	ΔS (kJ/mol $\cdot$ K)
AC	298	-23.97	8.17	0.11
	308	-24.93		
	318	-26.12		
WAC	298	-16.65	13.27	0.10
	308	-17.59		
	318	-18.65		
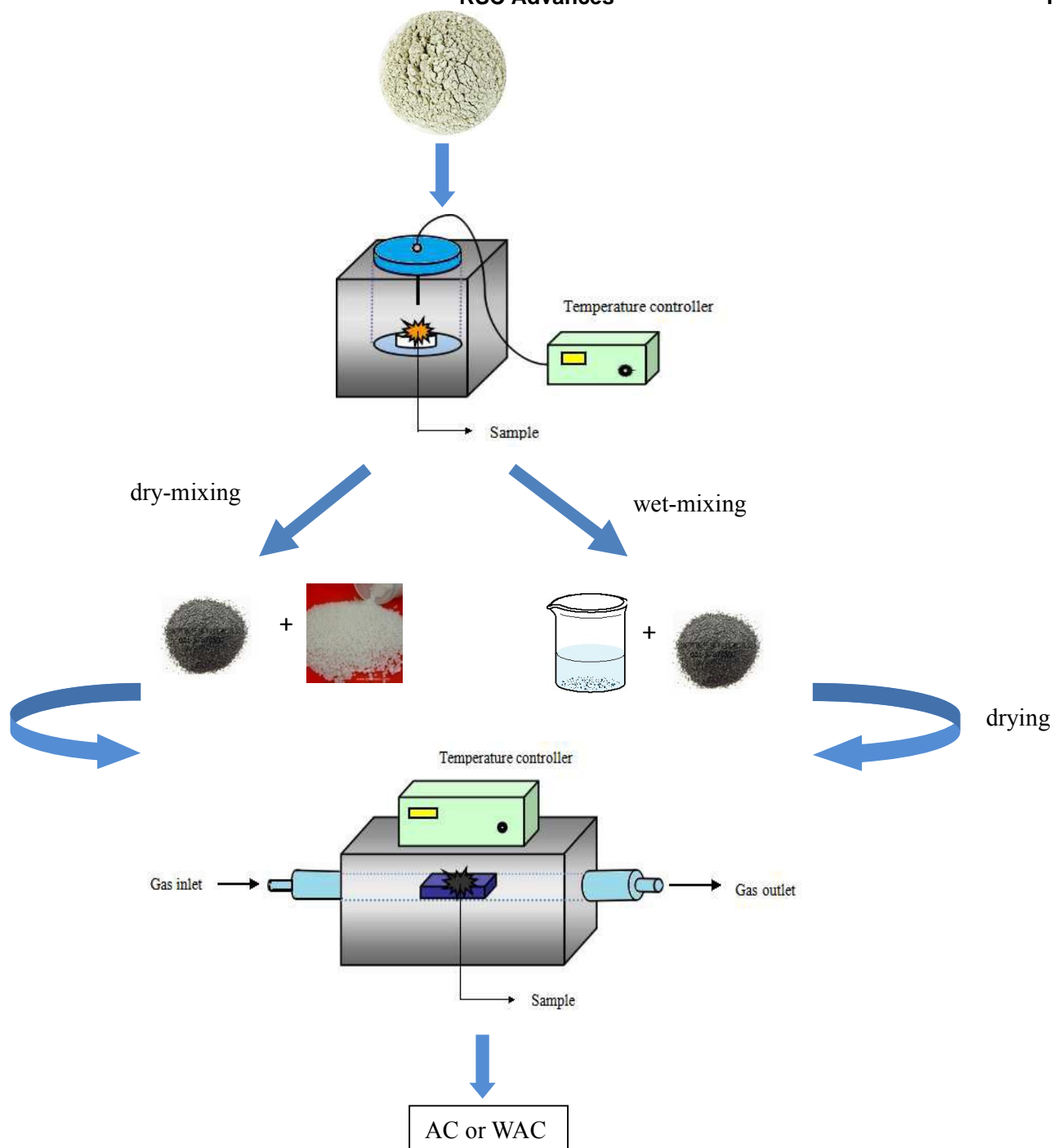
Two activated carbons have been produced from non-metallic fraction of waste printed circuit boards by NaOH activation in two methods, dry-mixing and wet-mixing. Dry-mixing is the waterless way by direct powder maceration. Wet-mixing is by impregnation within an aqueous solution, then the mixtures are dried at 110°C for 5 h. The NaOH/carbonized sample weight ratio is kept equal to 3:1. The activation heat-treatments are conducted under N_2 flow at 800 °C for 1 h in a cylindrical furnace. The carbon prepared by dry-mixing is named as AC. The carbon prepared by wet-mixing is named as WAC.